SECED 2023 Conference
Earthquake Engineering & Dynamics for a Sustainable Future
14-15 September 2023, Cambridge, UK

INFLUENCE OF CORROSION MODELLING STRATEGIES ON THE EXPECTED SEISMIC LOSSES OF A TYPICAL OLD ITALIAN RC BRIDGE

Nicola SCATTARREGGIA[1], Volkan OZSARAC[2],
Daniele MALOMO[3] & Ricardo MONTEIRO[4]

Abstract: *In Italy, as well as in many other countries, most old reinforced concrete (RC) bridges have reached their nominal lifespan, and recently observed bridge collapses clearly indicate they have seldom received proper and regular maintenance, which becomes an urgent matter now. Within such a context, analysing deteriorated RC bridges is rapidly and increasingly becoming the focus of national and international research. The corrosion of steel rebars, in particular, represents one of the major public safety threats, especially in seismic prone areas, considering it can further reduce the residual life/capacity of bridges designed prior to the introduction of modern codes including durability design prescriptions. In current performance-based assessment procedures for old RC bridges, corrosion modelling is considered in a very simplistic manner, often only reducing the area of rebars. To advance research in the field, this study assesses the impact of various modelling strategies on the risk assessment of a typical old RC bridge in Italy, also scrutinising different approaches of varying levels of detail, considering the reduction in yield/ultimate strength and ductility capacities of rebars, as well as of the concrete compressive strength. To this end, multiple-stripe analyses are carried out and fragility curves are developed using the various modelling approaches for various levels of corrosion. Finally, seismic losses are estimated and analysed to quantify the impact of the selected corrosion modelling approaches. Results show that the level of complexity adopted to model corrosion can produce differences in the structural response (i.e., moment-curvature capacity and fragility curves), whereas such differences reduce significantly in terms of expected annual losses.*

Introduction

In Europe, as in other regions worldwide, the age profile of RC bridges reflects the peak in construction after the Second World War (e.g., Iori and Poretti (2011)), which effectively implies that many of them are more than 50 years old - their typical nominal life. Nowadays most old bridges are also subjected to higher traffic demands with respect to those assumed during their original design, and are exposed more frequently to natural and human induced hazards that may cause failure (e.g., Imhof (2004)). This has led to a large stock of old bridges with reduced safety margins, as also shown by recently observed failures (see e.g., Scattarreggia, Salomone, *et al*. (2022); Scattarreggia *et al*. (2023)). The expected poor performance of old bridges is also exacerbated by the fact that they were not originally designed using modern design practices, but rather according to the limited level of knowledge of those times, and by the lack of proper maintenance and the exposure to climate change hazards (Calvi *et al.* 2019).

Within such context of ageing bridges, corrosion-induced damage is further reducing their lifespan at an alarming pace, which is already compromised by other concurrent factors, as demonstrated by the recent series of collapses that occurred in e.g., Asia (Tan *et al.* 2020) and South America (Diaz *et al.* 2009). Considering that bridges are the backbone of modern society infrastructure, while representing key components of transportation system and providing mutual connections among critical facilities, their out-of-service or collapse usually implies serious economic losses. Therefore, as highlighted in recent guidelines, e.g. CNR (2021), research is still needed to investigate progressive failure, resistance and robustness of deteriorated bridges, considering the interaction between continuous damage due to material degradation and discontinuous damage

[1] PhD, University School for Advanced Studies IUSS Pavia, Pavia, Italy, nicola.scattarreggia@iusspavia.it
[2] PhD, University School for Advanced Studies IUSS Pavia, Pavia, Italy
[3] PhD, McGill University, Montreal, Canada
[4] PhD, University School for Advanced Studies IUSS Pavia, Pavia, Italy

due to accidental events. Within such context, corrosion of steel rebars represents a major threat for old bridges, especially in seismically-prone countries.

As noted by e.g., Hanjari *et al.* (2011), corrosion processes affect the initial RC characteristics altering both the reinforcement, the steel-concrete bond as well as the surrounding concrete properties. Consequently, RC components experience a reduction of the mechanically-effective cross-section of reinforcement bars and a volume expansion that generates splitting stresses in the concrete, which may crack and spall the concrete cover, affecting the bond between reinforcement and concrete. As a result, corroded RC components subjected to external actions such as earthquake loadings, may be more vulnerable presenting a reduced strength and ductility capacity, as demonstrated by various experimental tests when comparing the performance of undeteriorated vs. deteriorated vertical load bearing components (e.g., Cheng *et al.* (2019)).

With the above in mind, the impact of various modelling strategies to account for corrosion-induced phenomena on the risk assessment of a typical old RC bridge in Italy is carried out by producing fragility curves and loss assessment. The different corrosion modelling strategies are tested within a fibre-based Finite Element model (FB-FEM) of the bridge, chosen for its balance between accuracy and computational time (e.g., Scattarreggia *et al.* (2021); Scattarreggia, Malomo, *et al.* (2022)). In addition to the simplified modelling strategy of cross-section reduction, the influence of the reduction in yield/ultimate strength and ductility capacities of rebars, as well as of the surrounded concrete compressive strength, is accounted for. To this end, multiple-stripe dynamic analyses are carried out and fragility curves are developed using the various modelling strategies for various levels of corrosion to characterise the bridge seismic damage. Finally, direct seismic losses are estimated and analysed to quantify the impact of the adopted corrosion modelling strategy.

Description of the case-study bridge

The case-study structure is a reinforced concrete bridge (Figure 1(a)) built in 1979, located in central Italy. The superstructure is constituted by five simply-supported spans, with a 12.5 m wide deck and five I-shaped girders with an average length of 34.6 m, placed at a spacing of 2.50 m from each other. The size of the expansion joints between adjacent spans and at abutments is 80 mm. The substructure consists of thin un-reinforced elastomeric bearings and piers with varying heights of 9.75 m, 13.4 m, 12.75 m and 10.22 m.

(a) **(b)**

Figure 1 (a) Photo of a portion of the bridge and (b) cross-section view of a pier.

The main cross-section characteristics of piers are shown in Figure 1(b). Specifically, they feature constant circular sections with a diameter of 2.6 m and compressive concrete strength of 29.1 MPa and all have 90 longitudinal rebars 34 mm of diameter (corresponding to longitudinal steel ratio of 1.6%) and circular hoops of 14 mm of diameter (corresponding to a transverse steel ratio of 0.055%), with the yield strength of 415.2 MPa. Shear keys with a 50 mm distance from girders are present on both cap beams and abutments, which restrains the movement in the transverse direction.

Numerical modelling

Bridge modelling

The adopted numerical model was developed in *OpenSeesPy* (Zhu *et al.* 2018), and it is shown in Figure 2. As deeply described in Ozsarac (2023), the connection between the substructure and superstructure was provided by a combination of bearings and shear keys (assumed to be non-sacrificial). The bridge deck was modelled by discretising each span with five elastic beam-column elements, whereas force-based beam-column elements were used for the bridge piers incorporating *P-Delta* effects. At the element ends, fibre sections were used whereas the linear elastic section with effective moment inertial properties derived from moment-curvature analysis of pier sections, were used at the element central portions. The plastic hinge lengths at the element ends were derived as proposed by Paulay and Priestly (1992). The Menegotto and Pinto (1973) relationship with 0.2% isotropic strain hardening was used for steel. The behaviour of concrete fibres follows the compressive stress-strain response proposed by Popovics (1973). The tensile strength was evaluated according to Collins and Mitchell (1991). The effect of confinement was accounted for thus strength and deformations were modified accordingly to distinguish confined fibres from those unconfined.

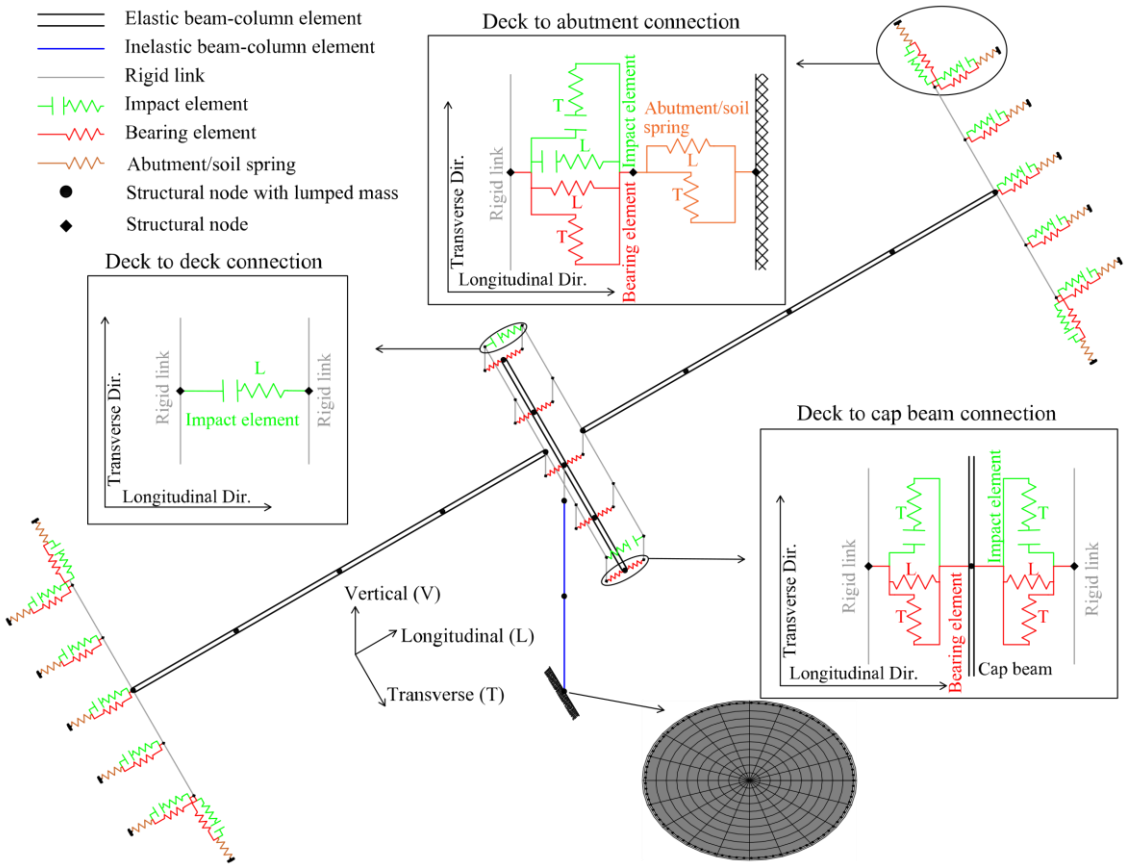

Figure 2 Schematic of the adopted numerical modelling strategy (from Ozsarac (2023)*).*

Although interested readers are referred to the work by Ozsarac (2023) for further modelling details, it is noted that impact elements were introduced in potential pounding locations, while bearings were modelled assuming coupled friction properties with a reference coefficient of 0.4 and assuming an initial stiffness proportional to the characteristic of the thin elastomeric bearings. Furthermore, foundation flexibility was not considered and fully-fixed supports for the piers were used. Abutments were assumed to contribute to bridge stiffness in both transverse and longitudinal directions accounting for the active and passive pressure of embankment directions, which modelling characteristics were defined according to Caltrans (2019) guidelines for the longitudinal direction and as recommended by Maroney and Chai (1994) for the transverse direction.

Corrosion modelling

As discussed by Hanjari *et al*. (2011) and similar to what was carried out by Scattarreggia *et al.* (2020) the effect of corrosion on concrete can be simulated by considering the removal of spalled concrete, reducing the section geometry, as well as considering the reduction of its mechanical properties around corroded reinforcement. For what concerns steel rebars, the reduction of cross-section area, ductility and yield and ultimate strengths may be considered. As result of geometrical and mechanical properties modifications of both concrete and reinforcement, their mutual interaction affects the bond through its degradation. In the present study, all mentioned phenomena were considered except for the bond degradation, given the intrinsic limitations of fibre-based idealisation where rebars are not explicitly modelled. The average corrosion penetration depth was assumed as a uniform volumetric mass loss, for both longitudinal and transverse reinforcement. The effect of confinement on concrete strength and deformation was accounted for according to the deteriorated properties of stirrups.

The corrosion level of the reinforcement is usually measured through mass loss (expressed in percentage and calculated as $1-(\phi'/\phi)^2$, where ϕ' is the corroded rebar diameter (Afsar Dizaj *et al.* 2018). The mass loss is usually the main parameter that, in combination with structural details characteristics, is used to calculate the additional parameters affected by corrosion (e.g., reduced yield strength) using relationships available in the literature, as usually adopted in FB-FEM applications (e.g., Rao *et al.* (2017); Cheng *et al.* (2019)). For instance, those derived by Shetty *et al.* (2015) for the reduced cross-section, (Coronelli and Gambarova 2004) for the degraded concrete properties, (Du *et al.* 2005) for the reduced yield strength of steel rebars and (Cairns *et al.* 2005) for the reduced ultimate strain of steel. It is noted that the ultimate strain of steel has been assumed to vary proportionally with the average cross-sectional loss, while a steel volumetric expansion of the corrosion products equal to 2 (as suggested by Afsar Dizaj *et al*. (2018)), with respect to uncorroded steel, has been used to calculate the reduced concrete compressive strength, similarly to what carried out by Scattarreggia *et al.* (2020).

Three levels of corrosion (expressed in terms of mass loss, as described above) have been assumed for the RC concrete piers of the analysed bridge, namely 5%, 15%, and 30%. The focus is on the difference between numerical results obtained when:

i. reducing only the rebars diameter (i.e., *X* - A_s, where *X* is the % of assumed mass loss);
ii. reducing both diameter and yield strength (i.e., *X* - A_s, f_{sy}); and
iii. reducing diameter and ultimate strain (and corresponding ultimate strength) of the steel in combination with the reduction of the compressive strength of the cover concrete (i.e., *X* - A_s, f_{sy}, ε_{su}, $f_{c,cover}$).

The preliminary comparisons in Figure 3 show the impact of such modelling options on the moment-curvature response of a RC pier of the case-study bridge, while it can be observed how the corrosion level reduced mostly the capacity.

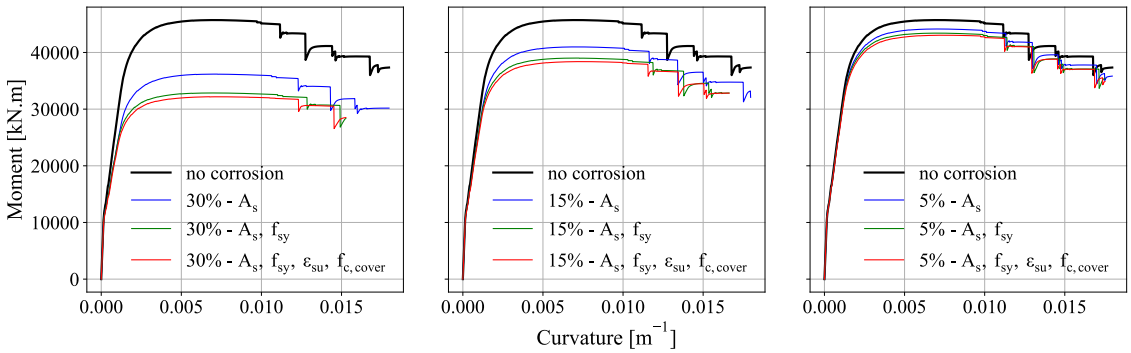

Figure 3 Moment-curvature analyses of the base section of a RC pier of the case-study bridge, considering various levels of mass loss corrosion-induced and modelling strategies of its effects.

A significant reduction is observed considering the sole reduction of the rebars area, while it slightly further reduces when also the mechanical properties of the materials are degraded (i.e., considering the modelling strategies that also include the reduction of yield strength of steel and its combination with a reduction of its ultimate strain and cover concrete strength). However, while

the reduction of the yield strength had a relevant influence on the capacity, both the corrosion-reduced ultimate strain of steel and the compressive strength of cover concrete seem to be of minor impact for the present case-study, given that it was the early failure of the concrete core that limited the structure/section ductility. Finally, it is noted that these observations apply to all of the three considered levels of corrosion (i.e., 30%, 15%, and 5% of mass loss), even if it, as expected, such differences are more evident when increasing the deterioration.

Seismic hazard characterization

Multiple-stripe analysis (MSA) was employed as the nonlinear dynamic analysis method to estimate the seismic response of the bridge. It yields 'stripes' of structural response values obtained by subjecting the structural model to sets of ground motion records matching multiple levels of the selected intensity measure (IM). Recent studies (O'Reilly 2021; Abarca *et al.* 2023) have shown that the average spectral acceleration (AvgSA) could be an efficient IM for predicting the response of multiple-span bridges such as the case-study bridge, which are prone to higher mode effects due to their inherent dynamic characteristics. In line with this, AvgSA was chosen as the IM to characterize the seismic hazard and was computed as per Equation (1):

$$AvgSA = \left[\prod_{i=1}^{n} SA(T_i)\right]^{1/n} \quad \text{where } T_i \in \left\{T_{lower}, T_{upper}\right\} \tag{1}$$

where T_{lower} and T_{upper} are the bounding periods, taken as 0.35 and 1.53, respectively, based on the bridge dynamic properties. Accordingly, these are equal to $T_{85\%}/1.5$ and $1.5\times T_1$, where $T_{85\%}$ is the geometric mean of periods corresponding to the cumulative modal participation of 85% in two principal horizontal directions, and T_1 is the geometric mean of fundamental periods in longitudinal and transverse directions.

The hazard curve for the considered site with V_{S30} of 400 m/s was obtained using the European Seismic Hazard Model 2013 (Woessner *et al.* 2015) whilst probabilistic seismic hazard analysis (PSHA) calculations were performed via OpenQuake (Pagani *et al.* 2014). For the computation of AvgSA, the indirect method proposed by Kohrangi et al. (2018) was followed utilising the ground motion model defined in Boore et al. (2014) and the correlation model proposed by Baker and Jayaram (2008). To ensure hazard consistency while selecting ground motion records, initially, the seismic disaggregation of hazard was performed at a total of 10 IM levels, corresponding to probabilities of exceedance ranging from 40% to 0.05% in 50 years (0.09g < IM < 1.70g), and the contributions of causal rupture characteristics (i.e., magnitude and Joyner-Boore distance) were identified. Then, as depicted in Figure 4, for each investigated IM level, a suite of records consisting of 30 ground motion pairs was selected from the NGA-West2 database (Ancheta *et al.* 2014) and scaled, using the EzGM toolbox (Ozsarac *et al.* 2023), to match the statistical distribution of the AvgSA-based conditional spectrum (Baker 2011; Kohrangi *et al.* 2017). For what concerns the correlations between the spectral ordinates at the different periods of vibration used for the computation of conditional spectra, the same model used in PSHA was adopted.

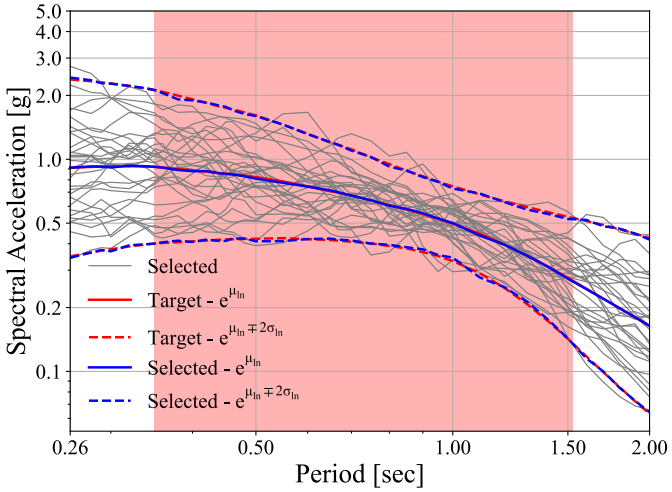

Figure 4 Comparison of target spectrum and spectra of selected ground motion records.

Seismic losses

The MSA results were used to compute the fragility curves for each component, assuming the response follows a lognormal distribution. Modelling uncertainty, component capacity uncertainty, and the dispersion due to record-to-record variability were assumed to contribute to the fragility curves total dispersion as carried out in Ozsarac (2023). For the case-study bridge, Figure 5 shows the obtained fragility curves for the above-described modelling strategies for three levels of mass loss, induced by corrosion: 30%, 15%, and 5%. The results show that for the lowest level of corrosion, i.e., 5%, the differences produced by the alternative modelling strategies are negligible, while they become more significant when increasing the intensity of corrosion. For the case associated with the 30% corrosion-induced mass loss, the results obtained by means of the simplified modelling of corrosion, i.e., reducing only the area rebars, are well aligned with those produced by the more refined modelling strategies for low IM levels, while differences become more noticeable for high IM levels because of the advanced nonlinear response of materials.

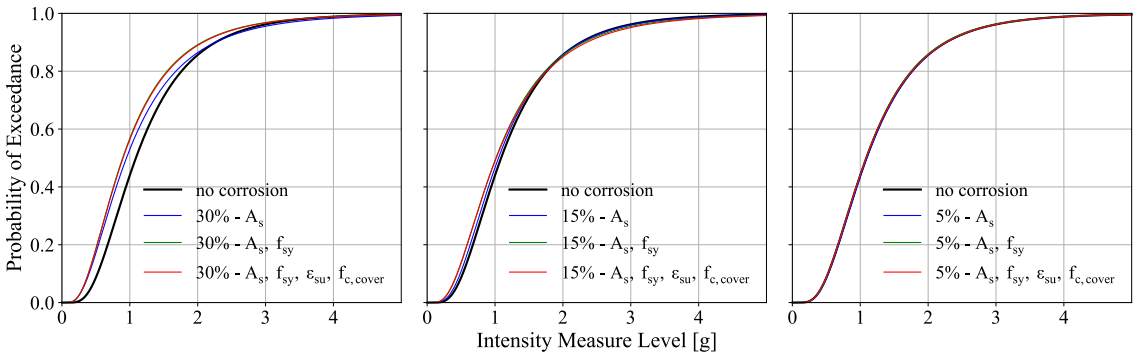

Figure 5 Fragility curves considering various levels of mass loss corrosion-induced and modelling strategies of its effects.

Damage models were then selected for the development of consequence models, based on the component damage models which relate the value of a given EDP (i.e., engineering demand parameter) with the probability P of a component entering a predetermined damage limit state (DLS), according to Perdomo and Monteiro (2020) and Perdomo, Abarca, *et al.* (2022) for cantilever circular RC columns and abutments, respectively. Subsequently, the consequence models were generated as the direct economic repair costs due to the attainment of expected damage, similarly to Perdomo (2020). In this regard, the repair actions, which require particular materials and tasks, were defined such that damage to the component is returned to its pre-earthquake (i.e., non-damaged) state. In specific, the repair and replacement costs were assumed to be lognormally distributed random variables with dispersion values of 0.4 and 0.5, respectively. Finally, the expected annual losses (EAL) were computed using a component level approach. Once the direct loss distribution at each IML was determined, the corresponding total expected loss values were computed and then integrated over the hazard curve to obtain the EAL. Figure 6 shows the loss curves for the case-study bridge, highlighting that the impact of corrosion on seismic losses can be seen mostly when using the simplified modelling strategy of only reducing the area of rebars, whereas no noticeable differences are found when using more refined modelling strategies that involve also the reduction of material mechanical properties (i.e. yield strength and ultimate strain of steel, as well as the concrete compressive strength around reinforcement). Overall, regardless of the relative impact of the specific modelling strategy adopted to account for the effect of corrosion on seismic losses, the results have highlighted the importance of their consideration for a more accurate assessment of expected losses (Figure 6), for levels of corrosion above 15%, which would otherwise be underestimated. Similar observations can be made from the expected annual losses normalised with respect to the mean bridge replacement cost (EALR), reported in Table 1.

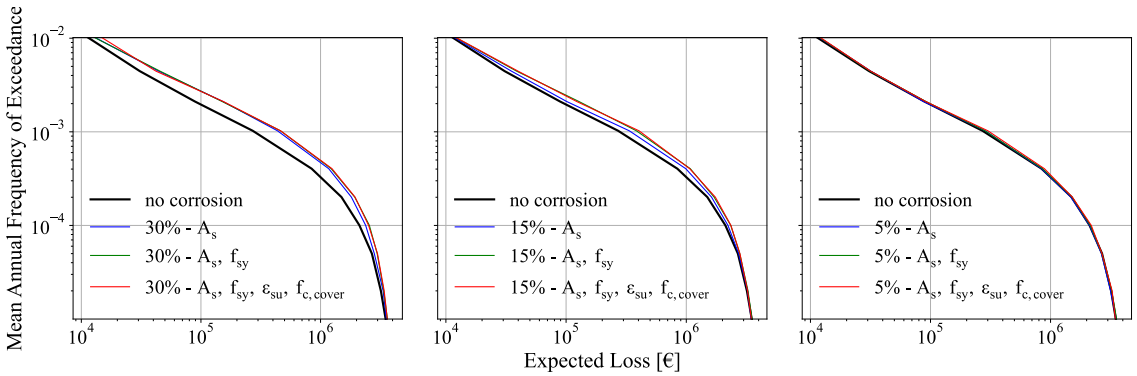

Figure 6 Expected loss curves considering of various levels of mass loss corrosion-induced and modelling strategies of its effects.

EALR	**Mass loss corrosion-induced**		
Modelling strategy	*30%*	*15%*	*5%*
no corrosion	0.035	0.035	0.035
A_s	0.047	0.039	0.035
A_s, f_{sy}	0.049	0.043	0.036
A_s, f_{sy}, ε_{su}, $f_{c,cover}$	0.050	0.043	0.037

Table 1. Expected annual loss ratio, considering various levels of mass loss corrosion-induced and modelling strategies of its effects.

Conclusions

In this work, the influence of typically-employed strategies for corrosion modelling on expected seismic losses of a typical old Italian RC bridge have been investigated using fibre-based FEM models. To this end, three modelling strategies of increasing complexity were considered, namely (i) the sole reduction of the rebars diameter, (ii) its combination with the corresponding reduction of yield strength, and (iii) further considering the reduction of the ultimate strain of steel (and associated ultimate strength) and the reduction of the concrete compressive strength of the fibres around reinforcement.

Preliminary moment-curvature analyses showed that the extent of expected impact of corrosion-induced phenomena increases with the complexity of the adopted modelling strategy. Indeed, the simplified corrosion modelling strategy of considering only the reduction of the rebars area, in general, overestimated the capacity, with respect to the more refined options (ii) and (iii), especially for high levels of corrosion. The noticeable differences observed in moment-curvature analyses between the different considered modelling strategies did not reflect as much when fragility curves were derived from multiple-stripe analyses. In this respect, results have shown that modelling strategies of increasing complexity that involve the reduction of mechanical properties of materials may be needed in case of high levels of corrosion (e.g., 30% of corrosion-induced mass loss in the present case-study). Further on, the computed expected annual losses (EAL) indicated, for the analysed case-study bridge, that the modelling strategy adopted to account for corrosion-induced effects becomes less relevant, as the differences became less evident. Notwithstanding, results have highlighted the importance of including the effects of corrosion for a more accurate assessment of EAL, especially for high levels of corrosion, which would otherwise be underestimated. On the other hand, it is envisaged that additional/alternative modelling strategies to account for the effects of corrosion, not investigated herein, such as bond degradation, should also be analysed. Finally, the impact of the corrosion modelling strategy on the estimated losses should be further explored considering a thorough characterisation of the different types of uncertainty associated with modelling, component capacity and record-to-record variability.

References

Abarca, A., Monteiro, R., O'Reilly, G., Zuccolo, E., and Borzi, B. (2023) 'Evaluation of intensity measure performance in regional seismic risk assessment of reinforced concrete bridge inventories', *Structure and Infrastructure Engineering*, 19(6), 760–778, available: https://doi.org/10.1080/15732479.2021.1979599.

Afsar Dizaj, E., Madandoust, R., and Kashani, M.M. (2018) 'Exploring the impact of chloride-induced corrosion on seismic damage limit states and residual capacity of reinforced concrete structures', *Structure and Infrastructure Engineering*, 14(6), 714–729, available: https://doi.org/10.1080/15732479.2017.1359631.

Ancheta, T.D., Darragh, R.B., Stewart, J.P., Seyhan, E., Silva, W.J., Chiou, B.S.J., Wooddell, K.E., Graves, R.W., Kottke, A.R., Boore, D.M., Kishida, T., and Donahue, J.L. (2014) 'NGA-West2 database', *Earthquake Spectra*, 30(3), 989–1005, available: https://doi.org/10.1193/070913EQS197M.

Baker, J.W. (2011) 'Conditional Mean Spectrum: Tool for Ground-Motion Selection', *Journal of Structural Engineering*, 137(3), 322–331, available: https://doi.org/10.1061/(asce)st.1943-541x.0000215.

Baker, J.W. and Jayaram, N. (2008) 'Correlation of spectral acceleration values from NGA ground motion models', *Earthquake Spectra*, 24(1), 299–317, available: https://doi.org/10.1193/1.2857544.

Boore, D.M., Stewart, J.P., Seyhan, E., and Atkinson, G.M. (2014) 'NGA-West2 equations for predicting PGA, PGV, and 5% damped PSA for shallow crustal earthquakes', *Earthquake Spectra*, 30(3), 1057–1085, available: https://doi.org/10.1193/070113EQS184M.

Cairns, J., Plizzari, G.A., Du, Y., Law, D.W., and Franzoni, C. (2005) 'Mechanical properties of corrosion-damaged reinforcement', *ACI Materials Journal*, 102(4), 256–264, available: https://doi.org/10.14359/14619.

Caltrans (2019) *Caltrans Seismic Design Criteria*, SDC version 2.0, Sacramento, CA.

Calvi, G.M., Moratti, M., O'Reilly, G.J., Scattarreggia, N., Monteiro, R., Malomo, D., Calvi, P.M., and Pinho, R. (2019) 'Once upon a Time in Italy: The Tale of the Morandi Bridge', *Structural Engineering International*, 29(2), 198–217, available: https://doi.org/10.1080/10168664.2018.1558033.

Cheng, H., Li, H.N., and Wang, D.S. (2019) 'Prediction for lateral deformation capacity of corroded reinforced concrete columns', *Structural Design of Tall and Special Buildings*, 28(1), e1560, available: https://doi.org/10.1002/tal.1560.

CNR (2021) *Guide to Design of Structures for Robustness*, ROME.

Collins, M.P. and Mitchell, D. (1991) *Prestressed Concrete Structures*, Englewood Cliffs, NJ: Prentice Hall.

Coronelli, D. and Gambarova, P. (2004) 'Structural Assessment of Corroded Reinforced Concrete Beams: Modeling Guidelines', *Journal of Structural Engineering*, 130(8), 1214–1224, available: https://doi.org/10.1061/(asce)0733-9445(2004)130:8(1214).

Diaz, E.E.M., Moreno, F.N., and Mohammadi, J. (2009) 'Investigation of Common Causes of Bridge Collapse in Colombia', *Practice Periodical on Structural Design and Construction*, 14(4), 194–200, available: https://doi.org/10.1061/(asce)sc.1943-5576.0000006.

Du, Y.G., Clark, L.A., and Chan, A.H.C. (2005) 'Residual capacity of corroded reinforcing bars', *Magazine of Concrete Research*, 57(3), 135–147, available: https://doi.org/10.1680/macr.2005.57.3.135.

Hanjari, K.Z., Kettil, P., and Lundgren, K. (2011) 'Analysis of mechanical behavior of corroded reinforced concrete structures', *ACI Structural Journal*, 108(5), 532–541, available: https://doi.org/10.14359/51683210.

Imhof, D. (2004) *Risk Assessment of Existing Bridge Structures*.

Iori, T. and Poretti, S. (2011) *Storia Dell'ingegneria Strutturale in Italia*, SIXXI 3. ed, Architettura e Costruzione.

Kohrangi, M., Bazzurro, P., Vamvatsikos, D., and Spillatura, A. (2017) 'Conditional spectrum-based ground motion record selection using average spectral acceleration',

Earthquake Engineering and Structural Dynamics, 46(10), 1667–1685, available: https://doi.org/10.1002/eqe.2876.

Kohrangi, M., Kotha, S.R., and Bazzurro, P. (2018) 'Ground-motion models for average spectral acceleration in a period range: Direct and indirect methods', *Bulletin of Earthquake Engineering*, 16(1), 45–65, available: https://doi.org/10.1007/s10518-017-0216-5.

Maroney, B.H. and Chai, Y.H. (1994) 'Seismic design and retrofitting of reinforced concrete bridges', in *Proceedings of 2nd International Workshop, Earthquake Commission of New Zealand*, Queenstown, New Zealand.

Menegotto, M. and Pinto, P.E. (1973) 'Method of Analysis for Cyclically Loaded R. C. Plane Frames Including Changes in Geometry and Non-Elastic Behavior of Elements under Combined Normal Force and Bending', in *Proceedings of IABSE Symposium on Resistance and Ultimate Deformability of Structures Acted on by Well Defined Loads*, 15–22.

O'Reilly, G.J. (2021) 'Seismic intensity measures for risk assessment of bridges', *Bulletin of Earthquake Engineering*, 19(9), 3671–3699, available: https://doi.org/10.1007/s10518-021-01114-z.

Ozsarac, V. (2023) *Integrated Evaluation of Earthquake-Induced Economic Losses for Multi-Span Reinforced Concrete Bridges*.

Ozsarac, V., Monteiro, R., and Calvi, G.M. (2023) 'Probabilistic seismic assessment of reinforced concrete bridges using simulated records', *Structure and Infrastructure Engineering*, 19(4), 554–574, available: https://doi.org/10.1080/15732479.2021.1956551.

Pagani, M., Monelli, D., Weatherill, G., Danciu, L., Crowley, H., Silva, V., Henshaw, P., Butler, L., Nastasi, M., Panzeri, L., Simionato, M., and Vigano, D. (2014) 'Openquake engine: An open hazard (and risk) software for the global earthquake model', *Seismological Research Letters*, 85(3), 692–702, available: https://doi.org/10.1785/0220130087.

Paulay, T. and Priestly, M.J.N. (1992) *Seismic Design of Reinforced Concrete and Masonry Buildings*, Seismic Design of Reinforced Concrete and Masonry Buildings, available: https://doi.org/10.1002/9780470172841.

Perdomo, C. (2020) *Direct Economic Loss Assessment of Multi-Span Continuous RC Bridges under Seismic Hazard*.

Perdomo, C., Abarca, A., and Monteiro, R. (2022) 'Estimation of Seismic Expected Annual Losses for Multi-Span Continuous RC Bridge Portfolios Using a Component-Level Approach', *Journal of Earthquake Engineering*, 26(6), 2985–3011, available: https://doi.org/10.1080/13632469.2020.1781710.

Perdomo, C. and Monteiro, R. (2020) 'Simplified damage models for circular section reinforced concrete bridge columns', *Engineering Structures*, 217, 110794, available: https://doi.org/10.1016/j.engstruct.2020.110794.

Popovics, S. (1973) 'A numerical approach to the complete stress-strain curve of concrete', *Cement and Concrete Research*, 3(5), 583–599, available: https://doi.org/10.1016/0008-8846(73)90096-3.

Rao, A.S., Lepech, M.D., Kiremidjian, A.S., and Sun, X.Y. (2017) 'Simplified structural deterioration model for reinforced concrete bridge piers under cyclic loading1', *Structure and Infrastructure Engineering*, 13(1), 55–66, available: https://doi.org/10.1080/15732479.2016.1198402.

Scattarreggia, N., Malomo, D., and DeJong, M.J. (2022) 'A new Distinct Element meso-model for simulating the rocking-dominated seismic response of RC columns', *Earthquake Engineering & Structural Dynamics*, available: https://doi.org/10.1002/EQE.3782.

Scattarreggia, N., Orgnoni, A., Pinho, R., Moratti, M., and Calvi, G.M. (2023) 'Failure analysis of the impact of a falling object on a bridge deck ', *Engineering Failure Analysis*, 148, 107229, available: https://doi.org/10.1016/j.engfailanal.2023.107229.

Scattarreggia, N., Qiao, T., and Malomo, D. (2021) 'Earthquake Response Modeling of Corroded Reinforced Concrete Hollow-Section Piers via Simplified Fiber-Based FE

Analysis', *Sustainability 2021, Vol. 13, Page 9342*, 13(16), 9342, available: https://doi.org/10.3390/SU13169342.

Scattarreggia, N., Salomone, R., Moratti, M., Malomo, D., Pinho, R., and Calvi, G.M. (2022) 'Collapse analysis of the multi-span reinforced concrete arch bridge of Caprigliola, Italy', *Engineering Structures*, 251, 113375, available: https://doi.org/10.1016/J.ENGSTRUCT.2021.113375.

Shetty, A., Venkataramana, K., and Babu Narayan, K.S. (2015) 'Experimental and numerical investigation on flexural bond strength behavior of corroded NBS RC beam', *International Journal of Advanced Structural Engineering*, 7(3), 223–231, available: https://doi.org/10.1007/s40091-015-0093-6.

Tan, J.S., Elbaz, K., Wang, Z.F., Shen, J.S., and Chen, J. (2020) 'Lessons learnt from bridge collapse: A view of sustainable management', *Sustainability (Switzerland)*, 12(3), 1205, available: https://doi.org/10.3390/su12031205.

Woessner, J., Laurentiu, D., Giardini, D., Crowley, H., Cotton, F., Grünthal, G., Valensise, G., Arvidsson, R., Basili, R., Demircioglu, M.B., et al. (2015) 'The 2013 European Seismic Hazard Model: key components and results', *Bulletin of Earthquake Engineering*, 13(12), 3553–3596, available: https://doi.org/10.1007/s10518-015-9795-1.

Zhu, M., McKenna, F., and Scott, M.H. (2018) 'OpenSeesPy: Python library for the OpenSees finite element framework', *SoftwareX*, 7, 6–11, available: https://doi.org/10.1016/j.softx.2017.10.009.